Chapter 7

α-Synuclein Intramolecular Aggregation Studies

7.1 ABSTRACT

Understanding the formation of α-syn protofibril can allow more profound discovery on the pathogenesis of Parkinson's Disease. An α-syn mutant, Y19/W39, was mixed with wild type and A30P α-syn. Aggregation was then induced at elevated temperature. The aim was to extract distance distributions of this fluorescent donor-acceptor pair during the aggregation event using fluorescence energy transfer. The effect of the point mutation A30P, which has been suggested in causing familial Parkinson's Disease, was also probed. Proteolysis of α-syn, possibly by the presence of bacteria, caused irreproducible aggregation, thus preventing extrapolation of D-A distances. Despite this, we have learned that the presence of A30P α-syn leads to a faster aggregation rate.

7.2 INTRODUCTION

Parkinson's Disease is characterized by the presence of Lewy bodies in the *substantia nigra* region in the brain.[1] A major component of the Lewy bodies is of α-syn.[2,3] Protofibrils have been known to be the toxic species that causes the aggregation event.[4-6] Therefore, in order to understand the pathogenesis of α-syn, it is crucial to provide thorough understanding on the structures of protofibrils. The goal of this study is to employ fluorescent energy transfer (FET) to study the change of distance distribution during the formation of these protofibrils. Trp is again utilized as the fluorescent donor and Tyr(NO_2) as an energy acceptor. Y19/W39 has been chosen as the donor-acceptor pair.

In this aggregation study, the D-A α-syn mutant was mixed with wild type and A30P mutant in a 1:15 ratio. The point mutation A30P was studied because it is one of the mutations linked to familial PD.[7,8] Other techniques, such as absorption, Trp fluorescence, thioflavin T (ThT) fluorescence, circular dichorism, and SDS-PAGE were also employed to monitor the progress of aggregation.

7.3 METHODS

Protein Preparation.

Any necessary mutations for α-syn were introduced through site-directed mutagenesis and confirmed with DNA sequencing. Proteins used for this study were expressed, purified, and nitrated according to protocols outlined in Chapter 1. The purified protein solutions were concentrated using Amicon YM-3 (molecular weight

cutoff 3 kD; Millipore) and stored at -80 °C until the day before the experiment. The protein solutions were then exchanged into filtered 100 mM NaP_i buffer (pH 7.4) using HiPrep Desalting 26/10 column by the FPLC. The protein solutions were then stored in the cold room (4 °C) until the experiment. The protein concentrations were then determined using UV-Vis. All the oligomeric materials were removed by filtration using YM-100 (molecular weight cutoff 100 kD; Millipore) prior to use.

Aggregation Experiment Setup.

16 × 125 mm (VWR) test tubes were utilized for the aggregation studies. Test tubes and magnetic stir bars were cleaned with freshly made *aqua regia*, and then washed thoroughly with Milli-Q water. The test tubes were subsequently dried under reduced pressure. Concentrated protein solutions were then added into these dried test tubes, along with a cleaned magnetic stir bar. All samples had a final protein concentration of 80 μM. For the Trp or Trp/Tyr(NO_2) mutants, each sample consisted of 5 μM of either the Y19/W39 or Y19/W39(NO_2). The rest of the proteins were furnished by WT or A30P. The test tubes were capped and incubated in a water bath shaker (New Brunswick Scientific) at 37 °C under 200 rpm.

Characterization of Aggregation Process.

Prior to withdrawing solutions from the aggregation samples, the test tubes were placed on the magnetic stir plate. The protein solutions were stirred gently for 5 min to allow even distribution of materials inside the test tubes. 200 μL aliquots of aggregation samples were withdrawn periodically for characterization.

Absorption of the protein solution was measured in a small-volume cuvette (200 μL) using a Hewlett-Packard 8452 diode array spectrophotometer. Trp fluorescence was measured following procedures outlined in Chapter 1. For ThT fluorescence studies, a 1 mM ThT stock was made. The ThT experimental sample consisted of 4 μL ThT stock, 20 μL protein solution, and 176 μL 100 mM NaP_i buffer. The absorption of this solution was measured. The steady-state fluorescence spectra between 420 nm and 680 nm (2 nm band pass, 0.5 s integration) were obtained by exciting the samples at 400 nm (1 nm band pass). An average of three scans for each sample was obtained to improve signal-to-noise ratio.

If aggregates were present, further studies were performed to investigate the soluble protein remaining in the sample. Turbidity of the samples can be characterized by the elevation of the baseline in the UV-Vis spectra. When that was observed, the samples were then spun at 16 100 × *g* for 1 hr. The supernatant solutions were removed and their absorption and fluorescent characteristics were then probed.

The protein solution was also subjected to CD analysis on Day 0 and 6, with experimental parameters outlined in Chapter 1. The original protein solutions and their supernatants were also studied under SDS-PAGE and size-exclusion chromatography on Day 6 and 9. The protein sample was applied to a Superdex 75/300 size exclusion column on a FPLC. The column was previously calibrated by a mixture of protein containing Bovine Serum Albumin, Ribonuclease A, Cytochrome *c*, and Aproprotein.

7.4 RESULTS AND DISCUSSIONS

UV-Vis.

The aggregation event was monitored by a variety of techniques. UV-Vis spectroscopy provides a good tool to determine the presence of aggregates. The formation of multimers can shift the baseline higher. From **Figure 7.1a**, it shows that the baseline was rather flat and uniform at the beginning of the aggregation experiment. However, by Day 3, **Figure 7.1b** demonstrates a wide range of baselines from all the samples, implying that different amount of aggregates were formed. It is also noticeable that the baselines for the same type of samples, such as WT + Y19(NO_2)/W39, also vary. Since it has been our assumption that introducing the Trp/Tyr(NO_2) mutants will not cause any changes in the aggregation event, all the WT containing solution should produce similar absorption at a certain time point. This is the first evidence that protein aggregation is not reproducible.

When aggregates were first obtained, protein solutions were centrifuged to obtain the supernatant. The resultant solutions were screened with UV-Vis and the concentrations were tracked throughout the time course of experiment. We expected that **Figure 7.2** would illustrate that supernatant concentration decreases as aggregation events increase over time. This result did not typically agree, hence implying that the protein aggregation events between samples are not reproducible. However, A30P containing samples have demonstrated a faster rate of aggregate formation. This could be evidence that the presence of the A30P mutation could potentially speed up aggregation.

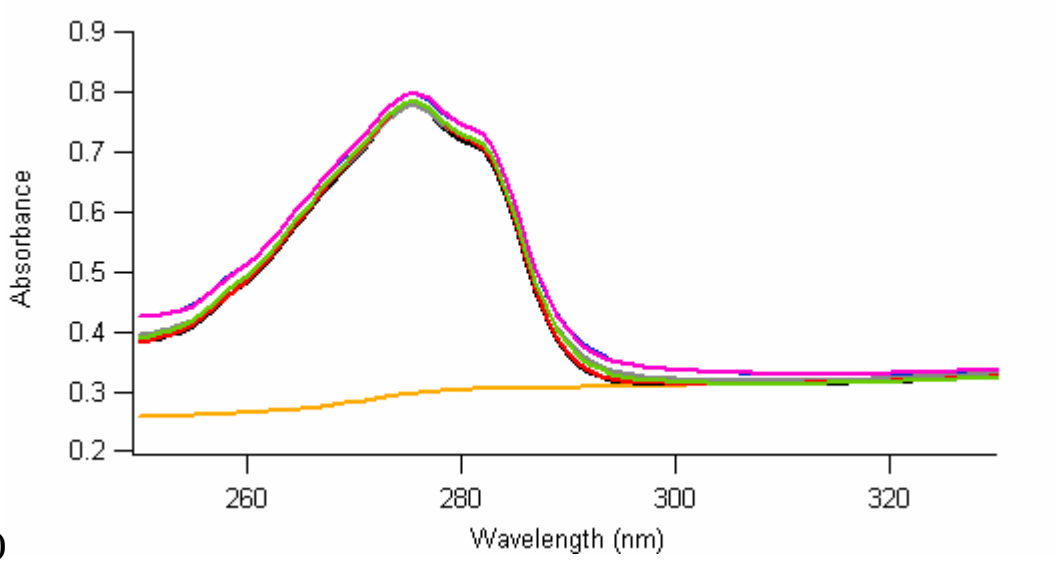

(a)

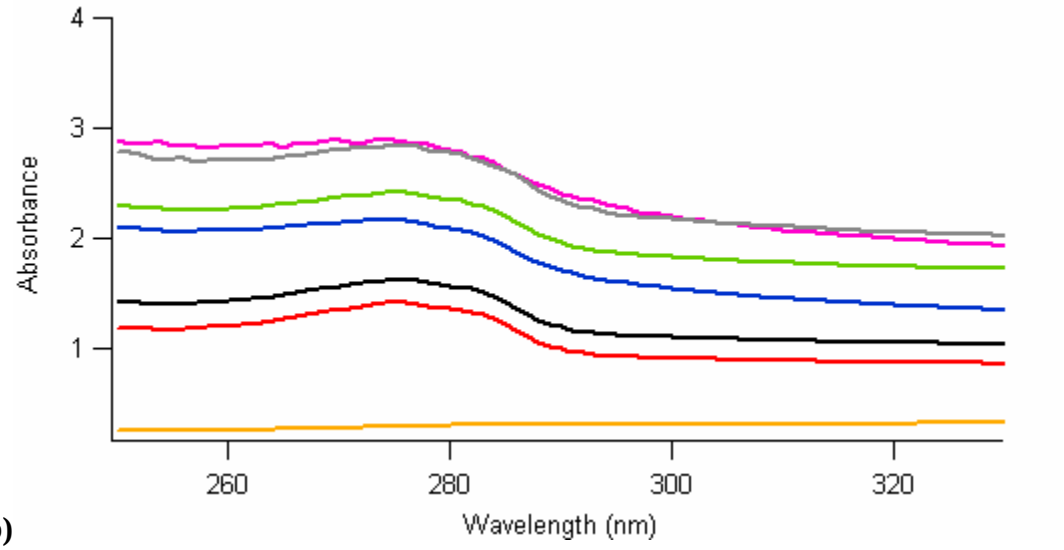

(b)

Figure 7.1. Absorption spectra of NaP_i buffer (orange), WT only (red), A30P only (black), WT + Y19/W39 (green), WT + Y19(NO_2)/W39 (blue or pink), and A30P + Y19/W39 (grey) at **(a)** Day 0 and **(b)** Day 3

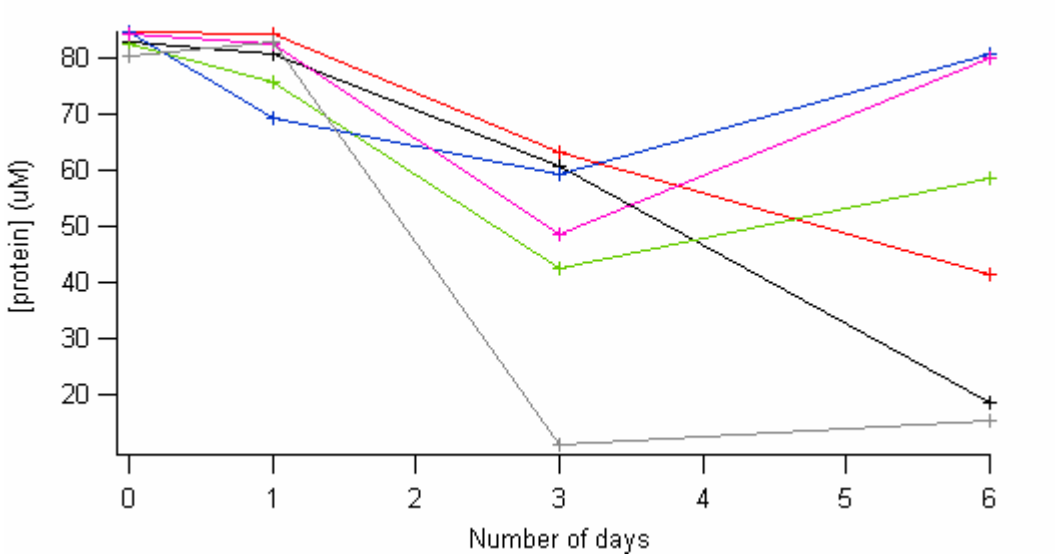

Figure 7.2. Supernatant protein concentration of WT only (red), A30P only (black), WT + Y19/W39 (green), WT + Y19(NO_2)/W39 (blue or pink), and A30P + Y19/W39 (grey) during the aggregation experiment, determined by UV-Vis spectroscopy

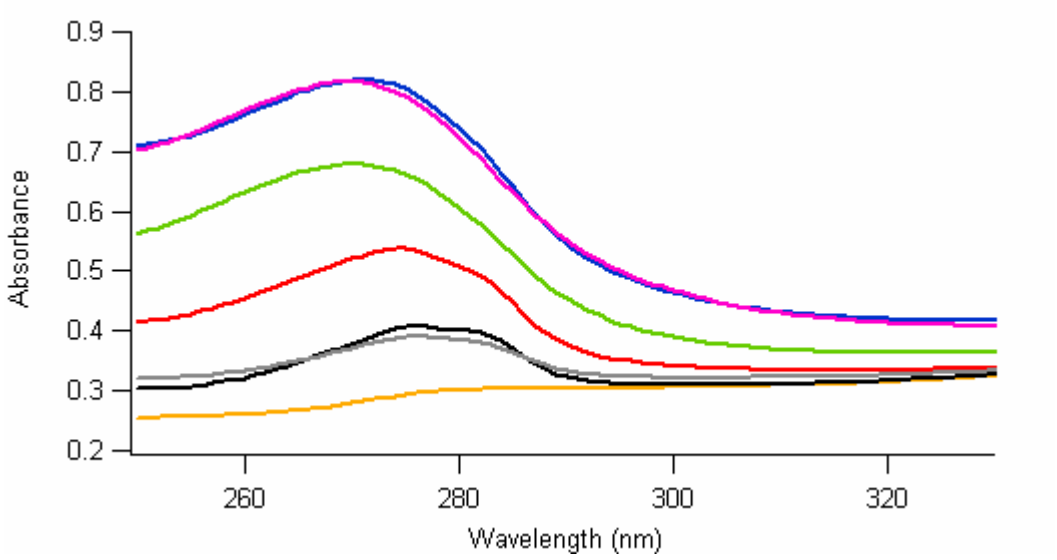

Figure 7.3. Absorption spectra for the supernatant of NaP_i buffer (orange), WT only (red), A30P only (black), WT + Y19/W39 (green), WT + Y19(NO_2)/W39 (blue or pink), and A30P + Y19/W39 (grey) at Day 6

Another interesting observation is that absorption traces between proteins in Day 0 (**Figure 7.1**) and the supernatants in Day 6 (**Figure 7.3**) are quite different. This could imply that protein materials in the supernatant in our experimental samples were altered during the aggregation event.

ThT Assay.

ThT is commonly known to bind to fibrils and exhibit birefringence.[9] Therefore, it is a common tool for characterizing the amount of fibrils during aggregation experiments.[10,11] **Figure 7.4a** illustrates that when ThT was mixed with monomeric α-syn, the emission was rather weak. After nine days of incubation, ThT emissions in all the samples became much more intense, by 10- to 40-fold (**Figure 7.4b**). This suggests that aggregates were developed during the incubation process.

However, the amount of ThT fluorescence within the WT-containing samples is not in agreement among each other. Similar phenomena have been observed for the A30P-containing samples, suggesting that the aggregation events studied here are not reproducible. This phenomenon can be further supported by **Figure 7.5**, where the normalized intensity has been plotted for individual samples to track the amount of aggregates formed over time. The rate of aggregation and the amount of aggregates formed are not uniform among samples.

As suggested by the results obtained by UV-Vis, A30P seems to form more aggregates at a faster rate. This can be confirmed with **Figure 7.4b**, as it displays that a higher ThT fluorescence was attained when A30P mutants were used. However, this faster aggregation rate cannot be conclusively verified by **Figure 7.5.**

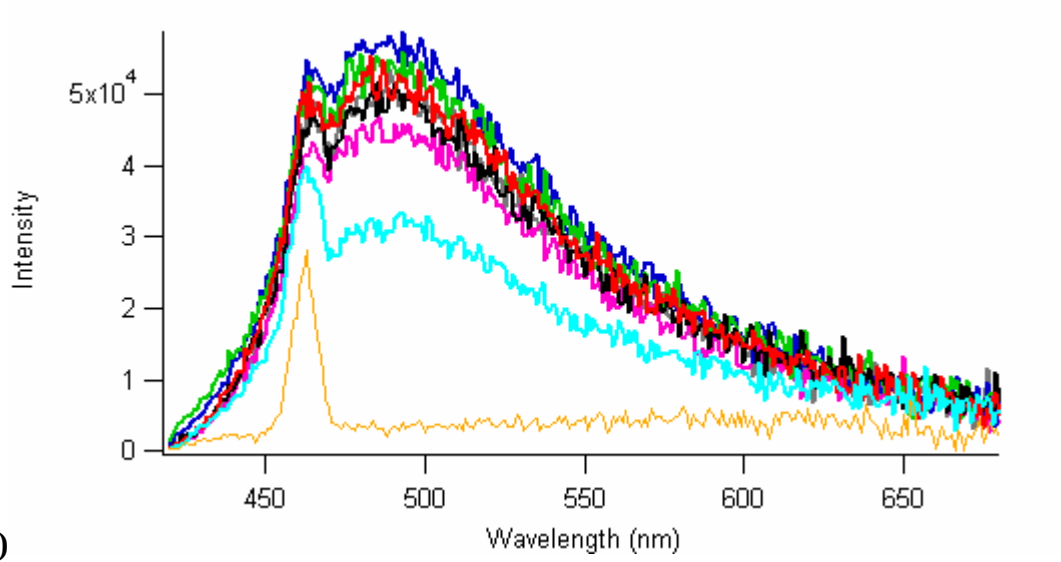

(a)

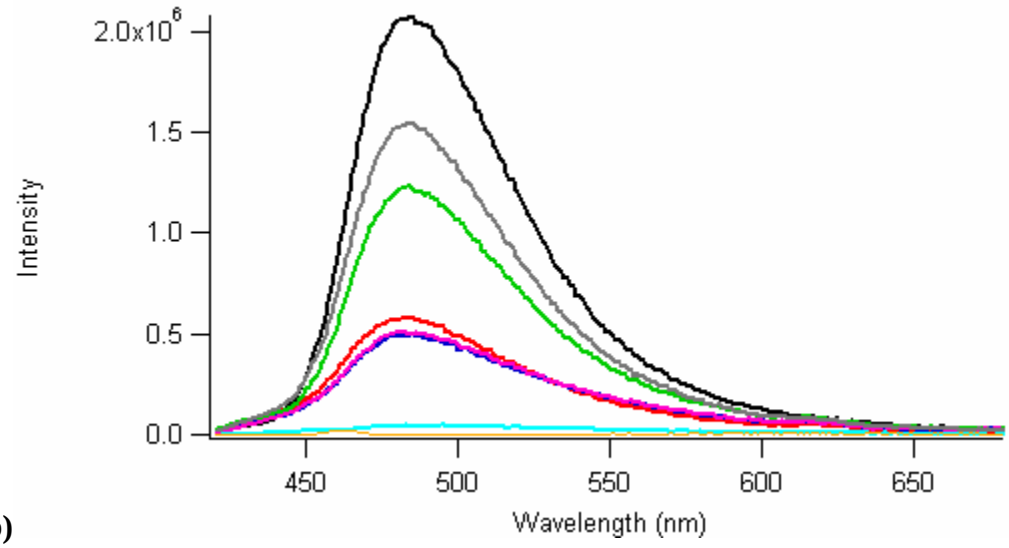

(b)

Figure 7.4. Thioflavin T fluorescence spectra of NaP_i buffer (orange), WT only (red), A30P only (black), WT + Y19/W39 (green), WT + Y19(NO_2)/W39 (blue or pink), and A30P + Y19/W39 (grey) at **(a)** Day 0 and **(b)** Day 9

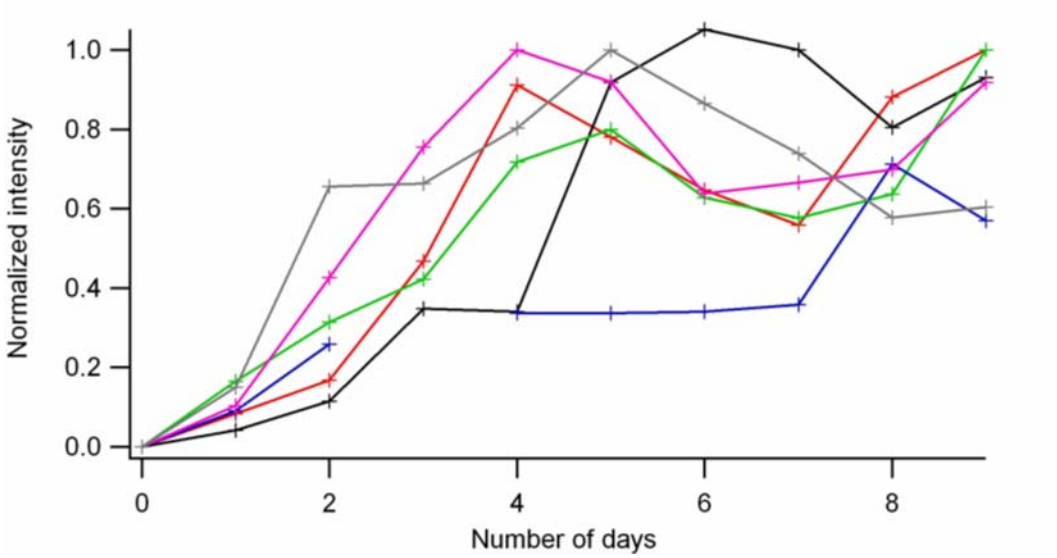

Figure 7.5. Normalized integrated intensity for the thioflavin T study for WT only (red), A30P only (black), WT + Y19/W39 (green), WT + Y19(NO_2)/W39 (blue or pink), and A30P + Y19/W39 (grey) throughout the aggregation study

Trp Steady-state Fluorescence Studies

As mentioned in previous chapters, Trp fluorescence is a powerful tool to investigate protein microenvironments.[12-15] Therefore, experimental samples were also subjected to Trp steady-state fluorescence studies to distinguish whether the W39 has become more buried as aggregation proceeds.

At the beginning of experiment, Y19/W39 samples exhibited higher fluorescence than samples containing Y19/W39(NO_2) because Trp fluorescence was quenched by the acceptor, 3-nitrotyrosine (**Figure 7.6a)**. The two samples (green and grey) containing Y19/W39 displayed comparable fluorescence, while similar emissions could be observed for samples with Y19/W39(NO_2). Even though no Trps were introduced in the WT-only and A30P-only samples, minimal fluorescence could still be observed due to minimal, though inefficient, Tyr excitation that could occur when samples were excited at 290 nm.

Figure 7.6b shows Trp fluorescence after nine days. The large increase of emission at 300 nm is mostly attributed to scattering caused by the aggregates. Trp fluorescence can be observed by the shoulder around 330 nm. Compared to the Trp emission in **Figure 7.6a**, at Day 9 we observe a higher emission, which is blue-shifted from λ_{max} = ~ 350 nm (Day 0) to ~ 330 nm (Day 9). As suggested in previous chapters, a higher fluorescence and blue-shifted λ_{max} suggest that the Trp is in a more hydrophobic environment. In this case, the Trps are now buried within the aggregates.

On the contrary, the Trp fluorescence for the supernatants (**Figure 7.6b**, dotted lines) at Day 9 are much weaker compared to the pre-centrifuged counterparts. Upon closer investigation (**Figure 7.7**), the λ_{max} (~ 340 nm) seems to be slightly blue-shifted compared to emission at Day 0. In addition, emission at ~ 450 nm can be observed,

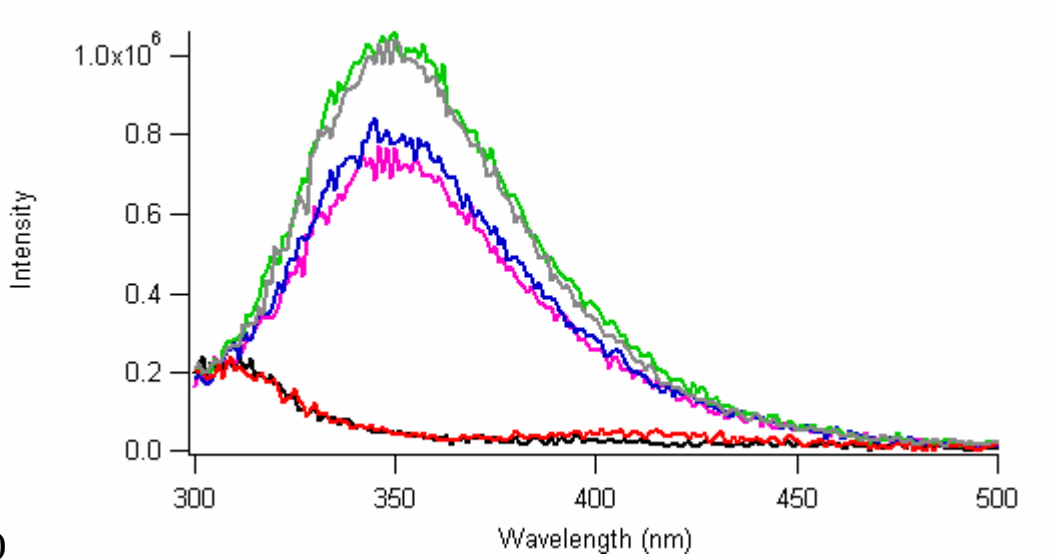

(a)

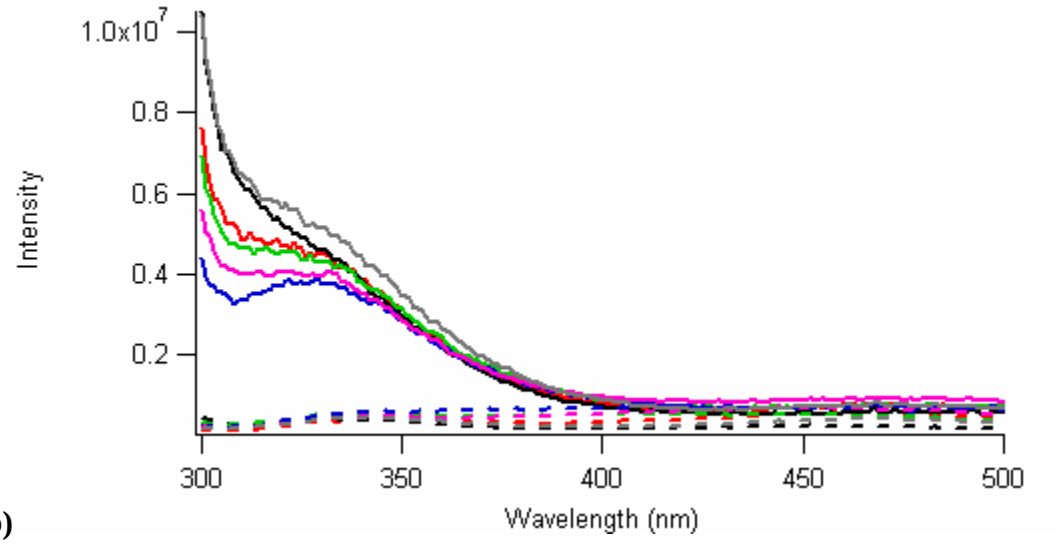

(b)

Figure 7.6. Steady-state fluorescence spectra of WT only (red), A30P only (black), WT + Y19/W39 (green), WT + Y19(NO_2)/W39 (blue or pink), and A30P + Y19/W39 (grey) at **(a)** Day 0 and **(b)** Day 9, along with spectra of their supernatants (dotted)

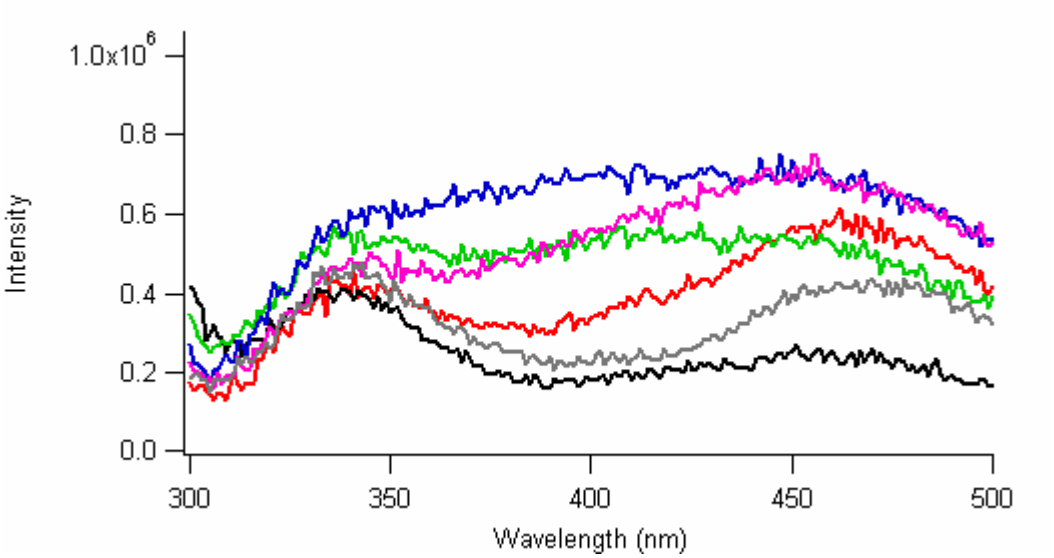

Figure 7.7. Steady-state fluorescence spectra of the supernatants for WT only (red), A30P only (black), WT + Y19/W39 (green), WT + Y19(NO_2)/W39 (blue or pink), and A30P + Y19/W39 (grey) at Day 9

suggesting the formation of a dityrosine linkage. Intermolecular tyrosine linkages may result in soluble multimers which remain in the supernatant. The presence of multimers can also bury the Trp, thus causing the blue-shift on the λ_{max}.

Circular Dichroism Experiments.

At the beginning of aggregation experiments, minimal structures were observed in the reaction mixtures (**Figure 7.8a**). After six days, **Figure 7.8b** shows that the reaction mixtures (dotted line) demonstrate a large increase of signal at ~ 218 nm, a signature peak of β-sheet formation,[16] implying aggregate formation. On the other hand, the CD signals obtained from the supernatant solutions show that the protein solutions were mostly unstructured (**Figure 7.8b**). Again, the discrepancies exhibited by similar samples show that the aggregation events studied were not reproducible.

SDS-PAGE Studies.

The reaction mixtures and their corresponding supernatants at Day 6 and Day 9 were subjected to SDS-PAGE studies (**Figure 7.9**). The monomer bands are highlighted by the arrows, showing that there were still some monomers remaining at those respective time points, with most of the monomers being consumed by Day 9. There were also more multimers shown in the SDS-PAGE from reaction mixtures on Day 9 than the corresponding SDS-PAGE from Day 6.

An interesting observation from the SDS-PAGE of the reaction mixtures from both days is that a species with a smaller molecular weight than the monomeric α-syn was present, suggesting that proteolysis may also occur during the aggregation process.

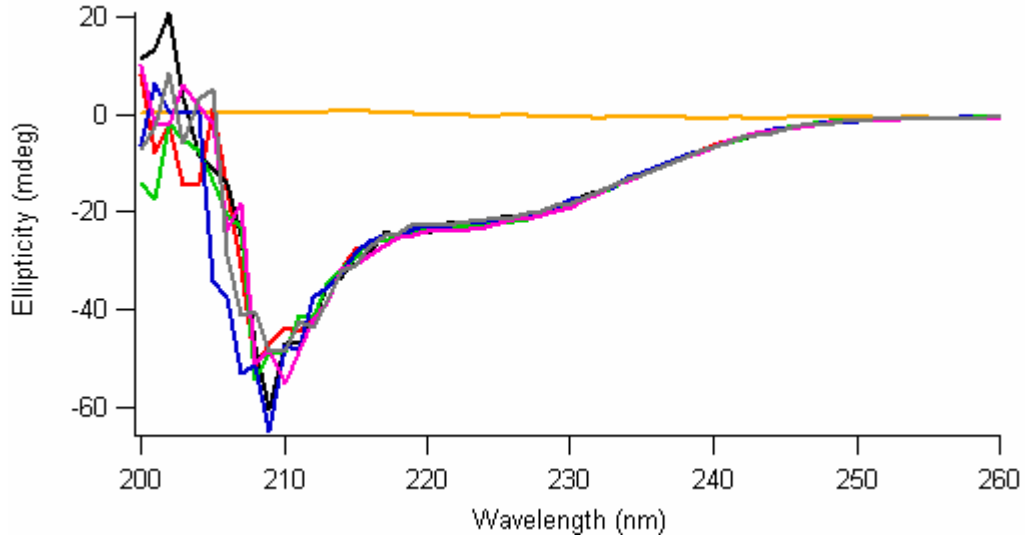

(a)

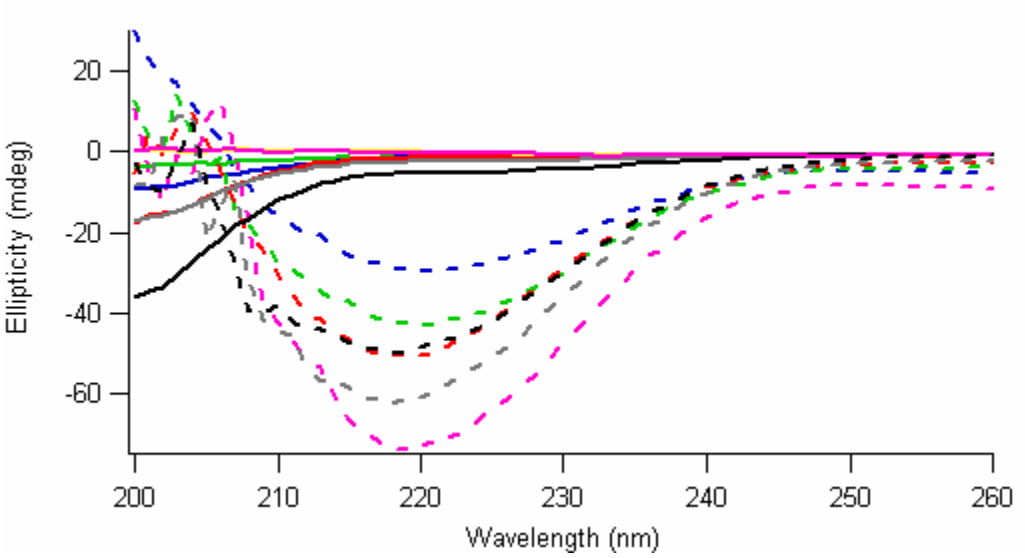

(b)

Figure 7.8. CD spectra at **(a)** Day 0 and **(b)** Day 6 of the reaction mixture (dotted) and supernatant (solid) from the following samples: NaP_i buffer (orange),WT only (red), A30P only (black), WT + Y19/W39 (green), WT + Y19(NO_2)/W39 (blue or pink), and A30P + Y19/W39 (grey)

(a)

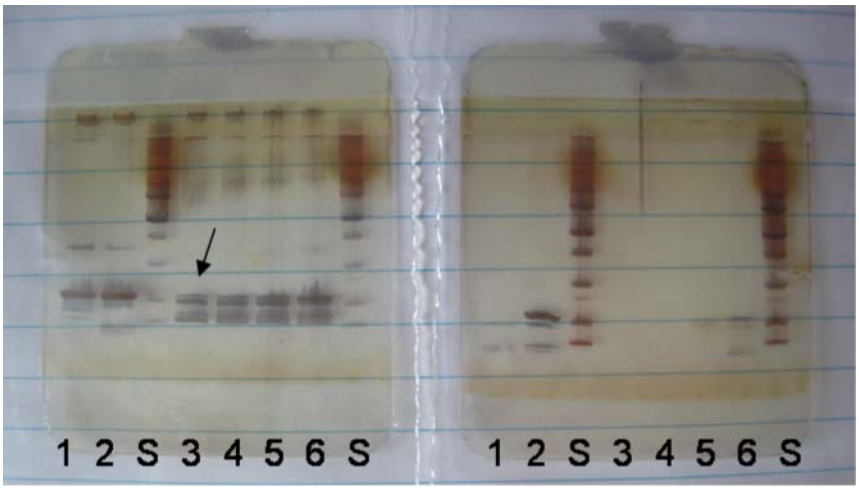

(b)

Figure 7.9. SDS-PAGE of WT only (lane #1), A30P only (lane #2), standard (lane #S), WT + Y19/W39 (lane #3), WT + Y19(NO_2)/W39 (lane #4 and #5), and A30P + Y19/W39 (lane #6) at **(a)** Day 6 and **(b)** Day 9 from reaction mixture (left) and supernatant (right). Monomeric species are indicated by arrows.

Size-exclusion Chromatography.

The aggregation mixtures from Day 6 and Day 9 were subjected to a size-exclusion column on a FPLC to separate the species in the reaction mixture according to their molecular weights. **Figure 7.10** shows these FPLC traces (red lines), along with the control (blue lines), consisting of Bovine Serum Albumin (67 kDa), Ribonuclease A (13.7 kDa), Cytochrome *c* (13.6 kDa), and Aproprotein (6.5 kDa). Since the heavier species eluted first, the peaks were assigned accordingly.

The most noticeable peak can be found after the 4th control peak, corresponding to the small aproprotein. This implies that the remaining species in the reaction mixture has a molecular weight smaller than 6.5 kDa, which is less than the 14 kDa α-syn monomer. This result further proves that proteolysis was present in the reaction mixture, giving rise to this small-molecular-weight species. This proteolysis process can be attributed to the presence of bacteria in the reaction mixture, digesting the protein during the aggregation event.

A shoulder peak corresponding to a species slightly smaller than 6.5 kDa can be observed from the reaction mixture in WT, but not in A30P. It seems that those species have been consumed in the A30P sample by this timepoint. In addition, although some of the large species can be observed in both traces, they are not dominant. Since all FPLC samples were filtered by a 220 nm filter before loading onto the size-exclusion column, it is highly likely that these high-molecular-weight species in the reaction mixture were filtered away.

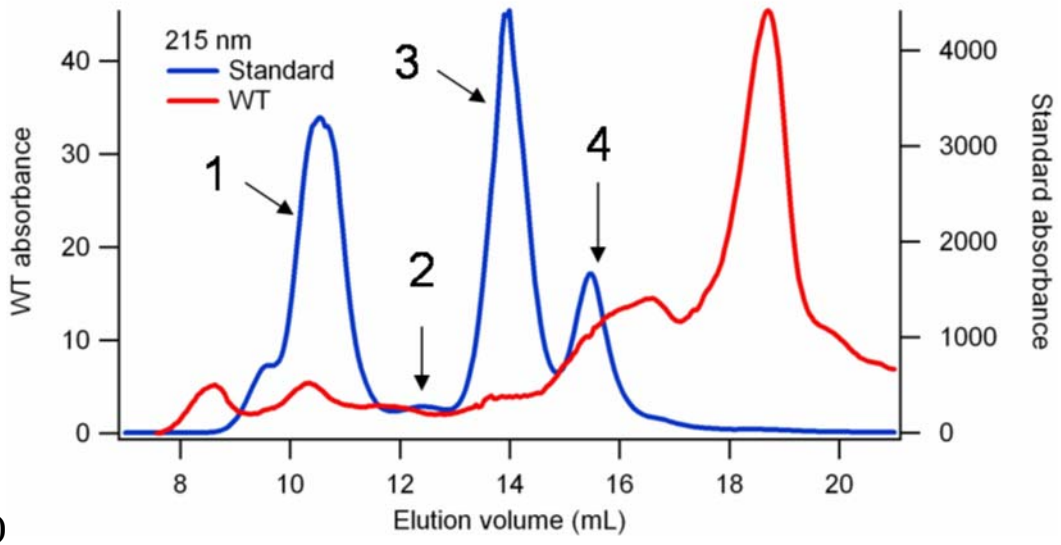

(a)

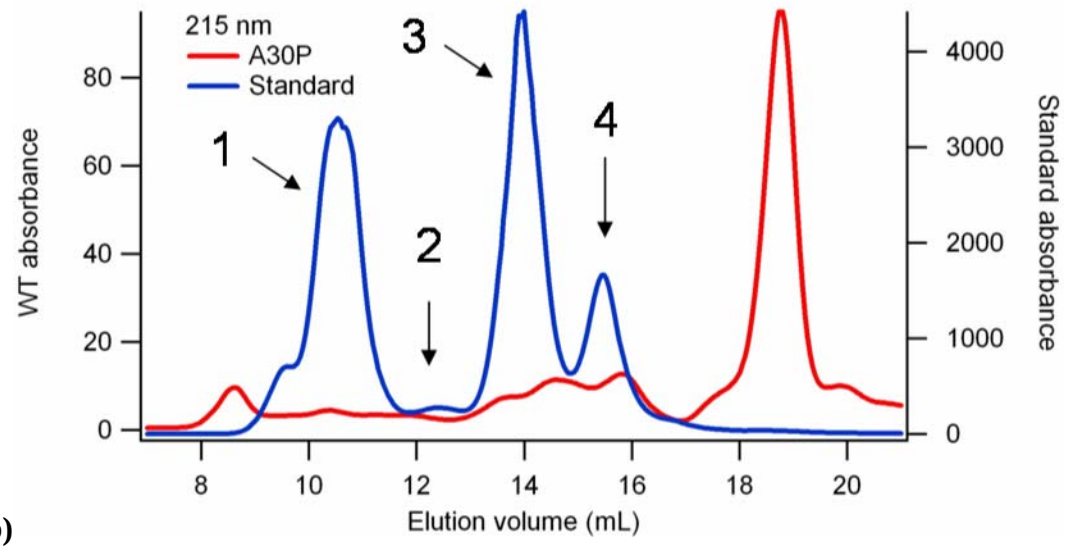

(b)

Figure 7.10. The FPLC traces of standards (blue), compared to the aggregation reaction mixture (red) from **(a)** WT only or **(b)** A30P only, using Superdex 75 10/300. The constituents of the standards are labeled by number, where 1 corresponds to Bovine Serum Albumin (67 kDa), 2 corresponds to Ribonuclease A (13.7 kDa), 3 corresponds to Cytochrome *c* (13.6 kDa), and 4 corresponds to Aproprotein (6.5 kDa).

Conclusion.

We have attempted to determine the change of intramolecular distance during the aggregation events of α-syn. However, it has been demonstrated that the aggregation process was not reproducible. Nonetheless, monitoring the aggregation of wild type and A30P α-syn protein in solution can provide some information on the formation of α-syn protofibrils. It is interesting to note that the aggregation rate for A30P mutants is faster than the wild type mutants. Also, proteolysis has been observed in the reaction mixture, possibly by the presence of bacteria, causing the irreproducible aggregation process. For future aggregation experiments, proteolysis could be prevented by introducing antibacterial agents in the aggregation mixture. Tools used in this study, such as CD, SDS-PAGE, size-exclusion columns, and ThT fluorescence studies, have been deemed appropriate for future α-syn aggregation experiments.

7.5 ACKNOWLEDGEMENTS

This project was completed in collaboration with Dr. Jennifer C. Lee.

7.6 REFERENCES

(1) Galvin, J. E.; Lee, V. M.; Schmidt, M. L.; Tu, P. H.; Iwatsubo, T.; Trojanowski *Adv. Neurol.* **1999**, *808*, 313–324.
(2) Spillantini, M. G.; Crowther, R. A.; Jakes, R.; Hasegawa, M.; Goedert, M. *Proc. Natl. Acad. Sci. U. S. A.* **1998**, *95*, 6469–6473.
(3) Spillantini, M. G.; Schmidt, M. L.; Lee, V. M. Y.; Trojanowski, J. Q.; Jakes, R.; Goedert, M. *Nature* **1997**, *388*, 839–840.
(4) Cookson, M. R. *Annu. Rev. Biochem.* **2005**, *74*, 29–52.
(5) Volles, M. J.; Lansbury, P. T. *Biochemistry* **2002**, *41*, 4595–4602.
(6) Zhu, M.; Li, J.; Fink, A. L. *J. Biol. Chem.* **2003**, *278*, 40186–40197.
(7) Kruger, R.; Kuhn, W.; Muller, T.; Woitalla, D.; Graeber, M.; Kosel, S.; Przuntek, H.; Epplen, J. T.; Schols, L.; Riess, O. *Nat. Genet.* **1998**, *18*, 106–108.

(8) Polymeropoulos, M. H.; Lavedan, C.; Leroy, E.; Ide, S. E.; Dehejia, A.; Dutra, A.; Pike, B.; Root, H.; Rubenstein, J.; Boyer, R.; Stenroos, E. S.; Chandrasekharappa, S.; Athanassiadou, A.; Papapetropoulos, T.; Johnson, W. G.; Lazzarini, A. M.; Duvoisin, R. C.; Di Iorio, G.; Golbe, L. I.; Nussbaum, R. L. *Science* **1997**, *276*, 2045–2047.
(9) LeVine, H. In *Amyloid, Prions, and Other Protein Aggregates* **1999**, *309*, 274–284.
(10) Roher, A.; Wolfe, D.; Palutke, M.; Kukuruga, D. *Proc. Natl. Acad. Sci. U. S. A.* **1986**, *83*, 2662–2666.
(11) Burns, J.; Pennock, C. A.; Stoward, P. J. *J. Pathol. Bacteriol.* **1967**, *94*, 337–.
(12) Reshetnyak, Y. K.; Koshevnik, Y.; Burstein, E. A. *Biophys. J.* **2001**, *81*, 1735–1758.
(13) Kleinschmidt, J. H.; den Blaauwen, T.; Driessen, A. J. M.; Tamm, L. K. *Biochemistry* **1999**, *38*, 5006–5016.
(14) Doring, K.; Konermann, L.; Surrey, T.; Jahnig, F. *Eur. Biophys. J.* **1995**, *23*, 423–432.
(15) Surrey, T.; Jahnig, F. *Proc. Natl. Acad. Sci. U. S. A.* **1992**, *89*, 7457–7461.
(16) Chiti, F.; Webster, P.; Taddei, N.; Clark, A.; Stefani, M.; Ramponi, G.; Dobson, C. M. *Proc. Natl. Acad. Sci. U. S. A.* **1999**, *96*, 3590–3594.